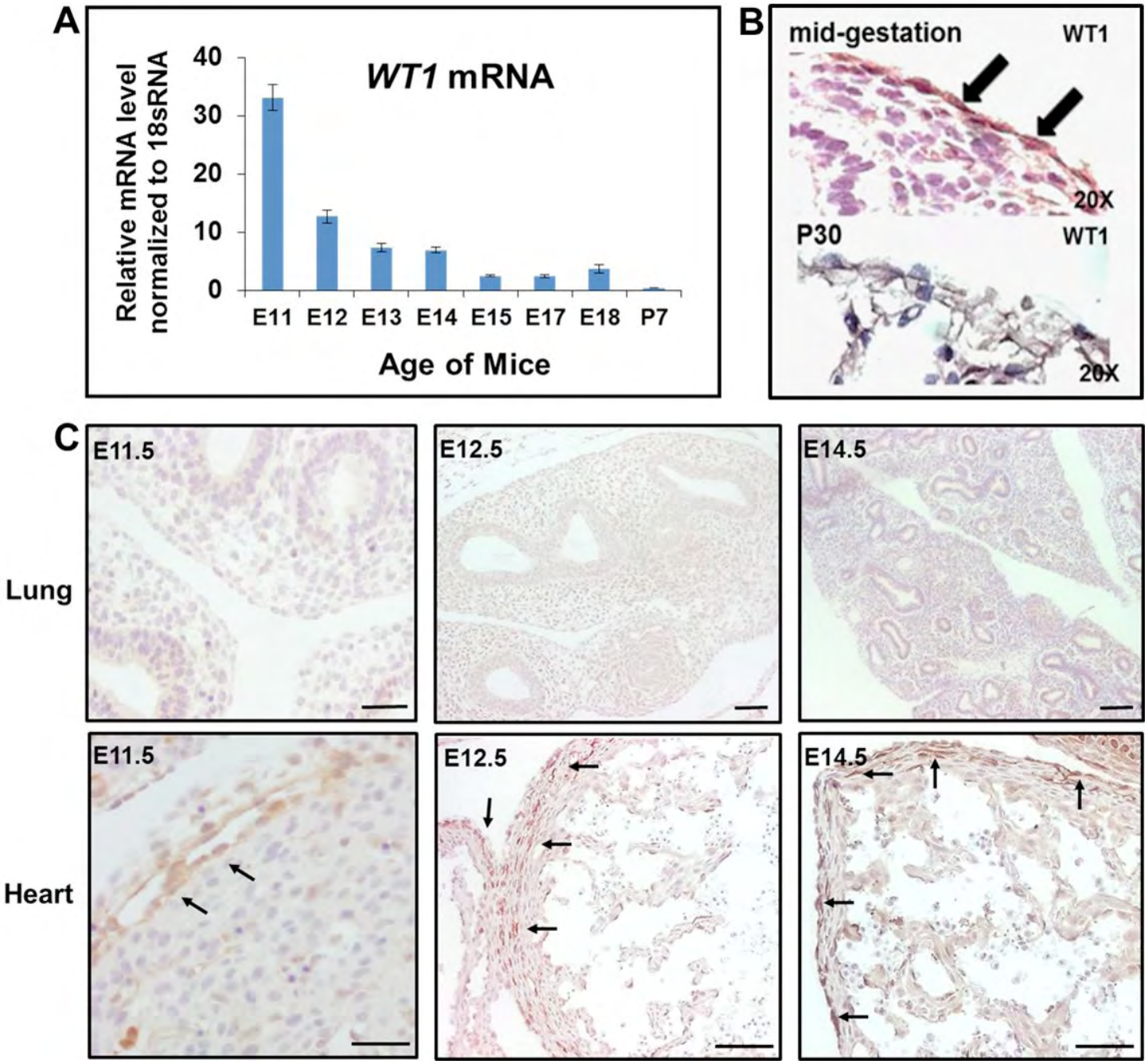

Fig. S1. Characterization of WT1 and mesothelin expression in mesothelial cells. (**A**) Temporal expression of *Wt1* mRNA in developing mouse lungs. Total RNA was extracted from whole lungs (including overlying mesothelium) of mouse embryos and postnatal day 7 (P7) pups before subjecting to qRT-PCR. Results were normalized to 18S rRNA. Data represent mean (± s.e.m.) from three mice for each age group. (**B**) Characterization of WT1 expression in *Rhesus macaque* lungs. WT1 immuno-labeling in mid-gestational (64 days) and neonatal (P30) *Rhesus macaque* lungs. WT1 protein is detected in fetal lung mesothelium (black arrow) but not in P30 lung. (**C**) Differential expression of mesothelin in the visceral mesothelium of the lung and the epicardium of the heart at E11.5, E12.5 and E14.5. Arrows point to mesothelin^{+} epicardial cells. Scale bars: 50 μm and 100 μm.

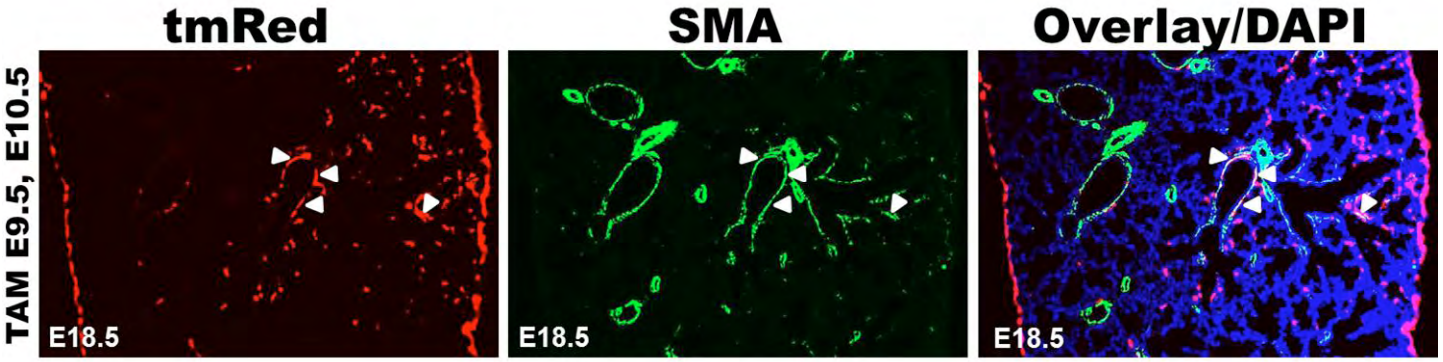

Fig. S2. Lineage tracing of fetal mesothelium at the time of lung bud formation. TAM was given at E9.5 and E10.5 to *Wt1*$^{CreERT2/+}$*;Rosa(tmRed)* mice and the lungs were examined at E18.5. (**A-C**) Colocalization of tmRed and α-SMA in a subset of BSM cells (arrowheads). Nuclei were counterstained with DAPI (Blue). Scale bars: 50 μm.

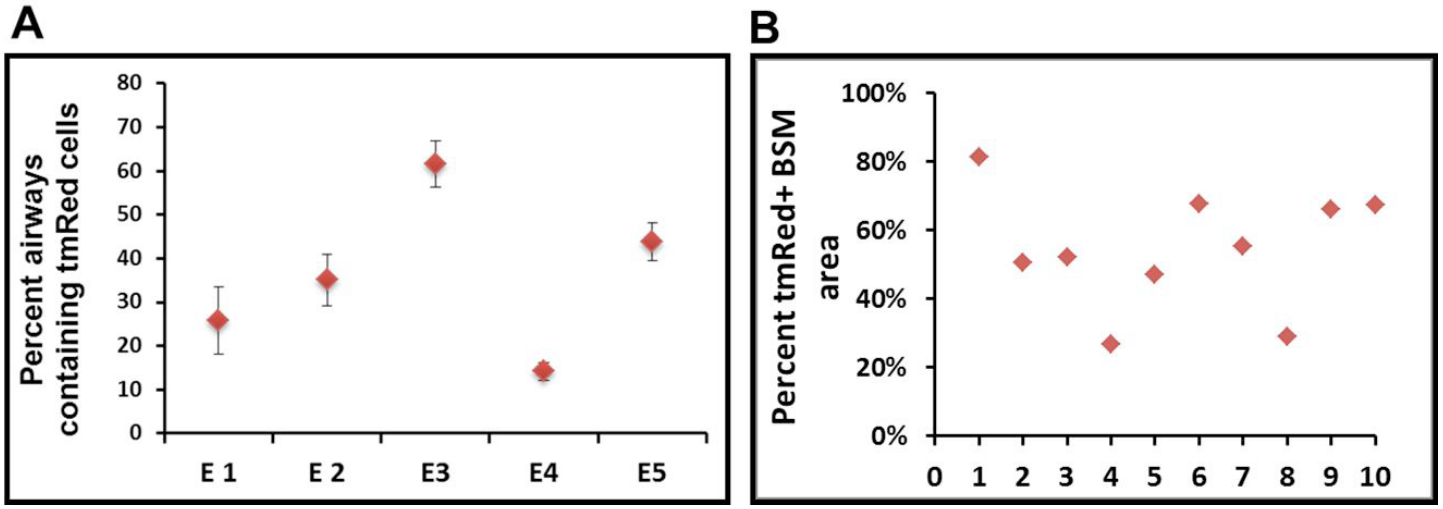

Fig. S3. Relative contribution of fetal mesothelium-derived airway smooth muscle. E18.5 tmRed^{+} lungs were isolated from *Wt1*$^{CreERT2/+}$*; Rosa(tmRed)* mice after TAM treatment at E10.5 and E11.5. Lungs were sectioned and immuno-labeled with an α-SMA antibody conjugated with FITC. **(A)** Percent airways that contained at least one tmRed^{+} BSM. Five embryonic lungs were analyzed with ten sections for each embryo. Data represent the average (± s.e.m.) for each embryo. E-Embryo. **(B)** Relative percent of the smooth muscle area around bronchi that is mesothelial-derived. ImageJ was used to quantify the total α-SMA immune-reactive area and the area that was concomitantly tmRed+. Ten airways from five mice were examined.

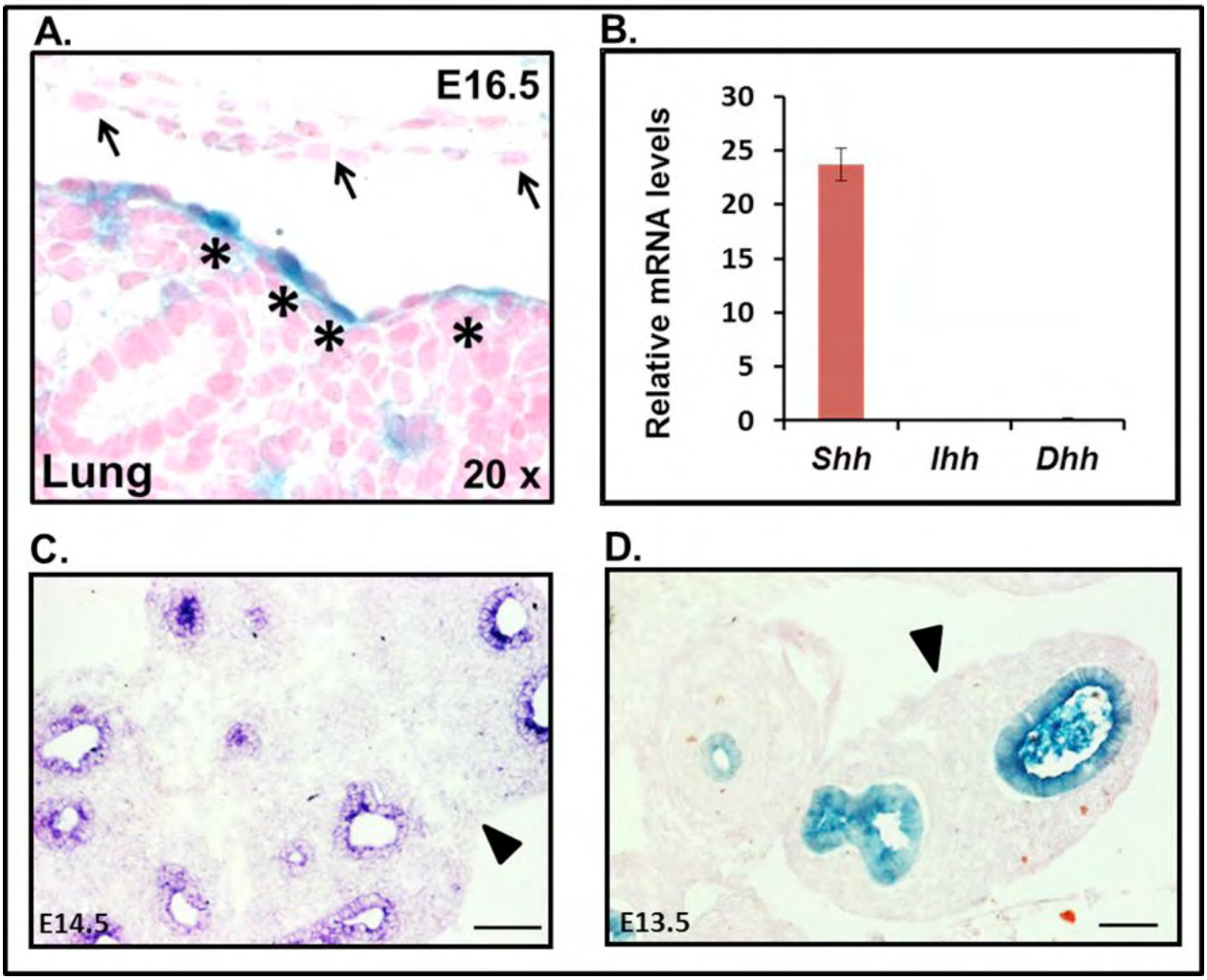

Fig. S4. Characterization of Hh signaling and Hh ligand expression in embryonic lung. (**A**) Differential Hh signaling activities in visceral and parietal mesothelium. Lungs were dissected from E16.5 *Gli1*$^{CreERT2/+}$*;R26RlacZ* mice after TAM injection at E12.5. Cells in visceral mesothelium expressed β-galactosidase (marked by asterisk *), indicative of active Hh signaling. In contrast, cells in parietal mesothelium (arrows) did not exhibit active Hh signaling, as indicated by a lack of β-galactosidase activity. Nuclei were stained with nuclear fast red. (**B**) Relative mRNA levels of *Shh, Ihh and Dhh* in E14.5 lungs as determined by qRT-PCR. Results were normalized to 18S rRNA. Data represent mean (± s.e.m.) from three different mice. (**C,D**) Expression of *Shh* in developing lung epithelium assayed by *in situ* hybridization at E13.5 (**C**) and by lineage labeling using *Shh*$^{Cre/+}$*;R26RlacZ* mice at E14.5 (**D**). No *Shh* expression was observed in visceral mesothelium (arrowheads). Scale bars: 50 μm.

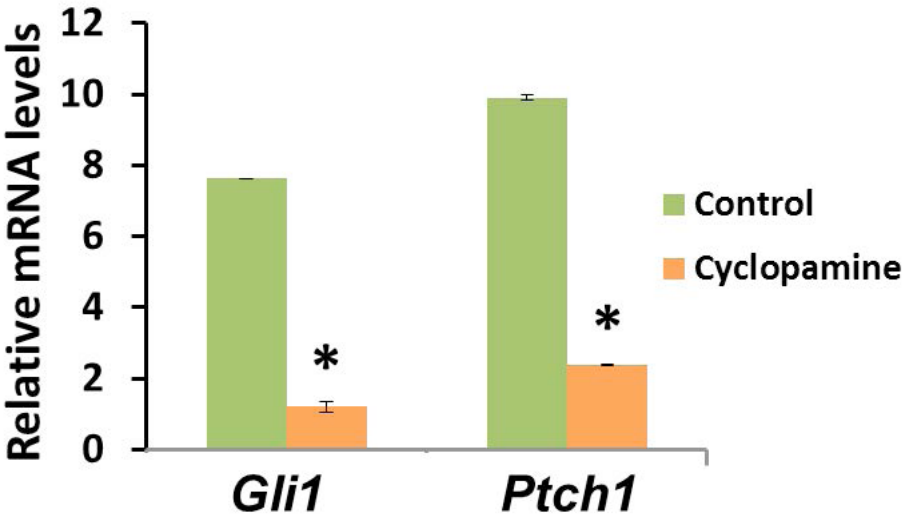

Fig. S5. Examination of Hh activity in lung cultures. E11.5 lungs were cultured in the presence of DMSO (vehicle) or 0.5 μM cyclopamine (Hh pathway inhibitor) for 48 hr before gene expression analysis of Hh pathway constituents *Gli1* and *Ptch1*. Results were normalized to 18S rRNA. Data represent mean (± s.e.m.) from three mice. *p<0.05.

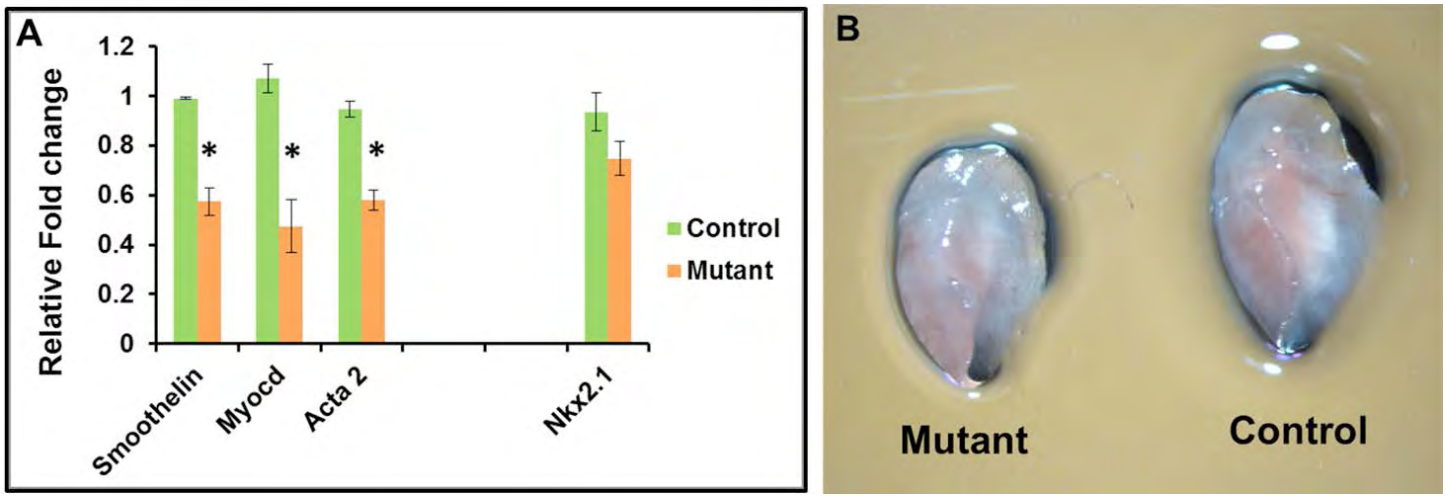

Fig. S6. Examination of the lung phenotype in mesothelial loss-of-Hh function mutant lungs. Lungs from *Wt1*$^{CreERT2/+;}$*Smo*$^{f/f}$ (mutant) and *Wt1*$^{CreERT2/+;}$*Smo*$^{f/+}$ littermate controls were analyzed at E14.5 and E18.5 after TAM administration at E10.5 and E11.5. (**A**) Mesothelial Hh loss-of-function mutant lungs exhibited reduced mRNA expression of smooth muscle specific genes including *Smoothelin, Myocd (myocardin),* and *Acta2* without any change in expression of the epithelium-specific transcription factor *Nkx2.1*. Results were normalized to 18S rRNA. Data represent mean (± s.e.m.) from three mice. *p<0.05. (**B**) Mice with mesothelial Hh loss-of-function had reduced lung size at E18.5. Left lobes of mutant and control lungs were shown.

Movie 1. Time-lapsed movie showing migration of mesothelial cells into the lung parenchyma. E12.5 lungs were isolated from TAM-treated *Wt1*$^{CreERT2/+}$*;Rosa(tmRed)* mice and cultured on transwell inserts for 24 hours before live imaging by confocal microscopy for 2.5 hours. Time-lapsed movie from a single Z-focal plane (corresponding to figure 2I-L) shows movement of tmRed^{+} cells from the surface mesothelium into the lung parenchyma over 150 minutes. Note, the gray contours of the underlying lung are due to transmitted light.

Movie 2. Time-lapsed movie showing inhibition of mesothelial cell entry by cyclopamine. E12.5 lungs were isolated from TAM-treated *Wt1*$^{CreERT2/+}$*;Rosa(tmRed)* mice and cultured for 24 hours in the presence of cyclopamine (Cyclo, 0.5 μM) before imaging for 2.5 hours. Time-lapsed movie from a single Z-focal plane (corresponding to figure 5C-F) shows no mesothelial cell migration over 150 minutes. Note, the gray contours of the underlying lung are due to transmitted light.